Transactions, **SMiRT-26**
Berlin/Potsdam, Germany, July 10-15, 2022
Division V

NONLINEAR SEISMIC CAPACITY EVALUATION OF A REACTOR BUILDING

Adam Fila[1], Bojan Radmanović[2], Vladimir Ninčić[3], Tobias Richter[4], Antonin Colau[5], Andrii Nykyforchyn[6], Sunay Staeuble-Akcay[7]

[1] Senior Expert Engineer, Framatome GmbH, Karlstein, Germany
[2] Project Engineer, Framatome GmbH, Karlstein, Germany
[3] Expert Engineer, Framatome GmbH, Karlstein, Germany
[4] Principal Engineer, Framatome Inc., San Jose, CA, USA
[5] Engineer, Géodynamique et Structure, Montrouge, France
[6] Director Deterministic Safety Analyses, NPP Gösgen, Däniken, Switzerland
[7] Senior Earthquake Engineer, NPP Gösgen, Däniken, Switzerland

ABSTRACT

This paper presents a nonlinear static seismic capacity evaluation of the Gösgen reactor building. Thereby, nonlinear material behavior including local inelastic effects of the reinforced concrete elements are considered. In the analysis the equivalent seismic loads based on mass proportional loading are incrementally applied until the structural capacity is reached. At the review level earthquake for the site, it is determined that sufficient structural capacity exists in all the critical structural members once a load redistribution in the structure has taken place. Structural performance beyond the review level is also assessed through the HCLPF capacity. It is remarkable that the reactor building has an elastic margin large enough to resist a review level earthquake that is 2.7 times larger than the original design earthquake with more elastic margin beyond that. The inclusion of inelastic behavior returns an even larger beyond design capacity.

INTRODUCTION

As a result of the Fukushima Daiichi nuclear accident the Swiss Federal Nuclear Safety Inspectorate (ENSI) requested the nuclear power plants (NPP) in Switzerland to review their structures, systems, and components against an increased seismic hazard. The PEGASOS refinement project (PRP) - a recent extensive seismic hazard assessment performed for the Swiss utilities under the guidance of swissnuclear (association of the Swiss NPP operators) - and an updated ground motion prediction model by the Swiss Seismological Service (SED) formed the basis for the new “ENSI-2015” consistent ground motions.

The design of the Gösgen nuclear power plant started in 1966 and it was put into commissioning and commercial operation in 1979. The seismic design of the NPP was based on the deterministic hazard assessment approach based on the design basis earthquake (DBE) referenced to the horizontal peak ground acceleration (PGA). In 2016 based on the site-specific probabilistic safety hazard analysis (PSHA), new hazard assumptions were determined resulting in the median-centered ENSI-2015 uniform hazard spectrum (UHS) at the free-field ground surface with an increased horizontal PGA at annual exceedance probability (AEP) of $10^{-4}/a$ and significant increase of the spectral accelerations at frequencies above approx. $2Hz$ (Figure 1).

The new review level earthquake (RLE = ENSI-2015 UHS at $10^{-4}/a$) with a 2.7 times larger seismic hazard compared to the DBE provided a basis for the reassessment of the seismic safety at the Gösgen NPP (Figure 3). Thereby, deterministic safety analyses to assure the safe shutdown of the NPP and the compliance with radiological limits, as well as an update of the seismic probabilistic safety analysis (PSA) for re-evaluation of the contribution of seismic initiating events to plant operational risk are performed.

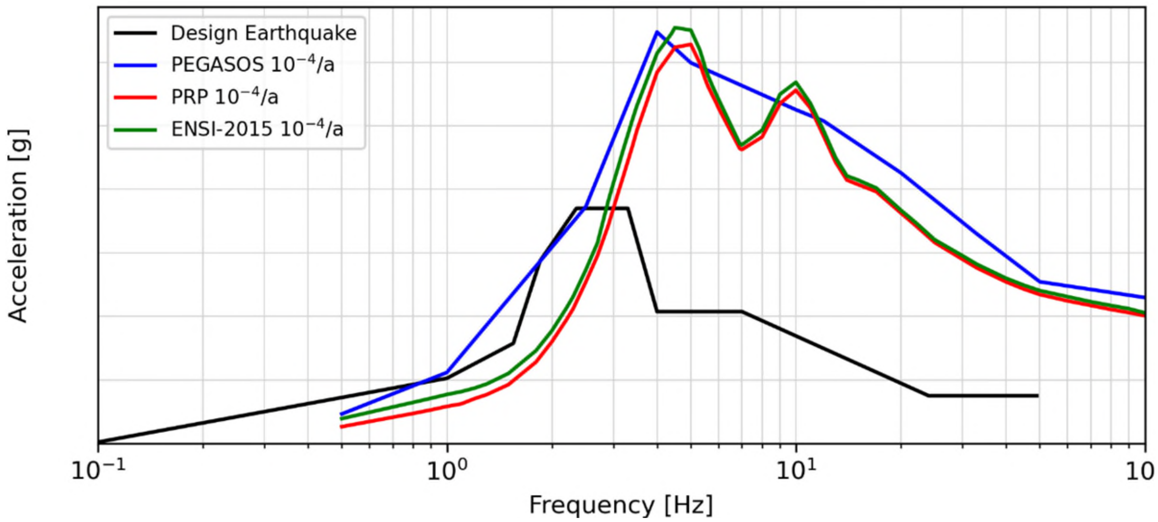

Figure 1. Comparison of Gösgen NPP uniform hazard spectra (mean) for AEP of 10^{-4}.

In the first part of the structural deterministic safety reassessment analysis, a response spectrum analysis (RSA) is performed to evaluate the reactor building structural demands at the RLE and to compare them with the allowable structural member capacities. This linear analysis did not show enough seismic margin with respect to the RLE demand. To increase the seismic margin and reduce conservatism as well as to realistically estimate post-elastic capacities of the critical structural members and the redistribution of the internal forces, a nonlinear static seismic capacity analysis is performed with a focus on the most critical structural members as determined by the RSA. Seismic structural performance beyond the RLE is also assessed through the HCLPF capacity. This is discussed in more detail in the following.

ELASTIC SEISMIC RESPONSE SPECTRUM ANALYSIS

Figure 3 shows the layout of the reactor building with relevant structural members. The primary lateral load resisting system is comprised of an exterior cylindrical wall, circular reactor building core, and cylindrical internal shielding wall. Radially positioned internal walls with thicknesses ranging from $0.3m$ to $1m$ are uniformly distributed over the perimeter.

Seismic response spectra used as a basis for the seismic response spectrum analysis are developed from the ENSI-2015 UHS at an AEP of $10^{-4}/a$ considering the kinematic soil-structure interaction (SSI) effects (kinematic input motions, KIM). Resulting translational (see Figure 2) and rotational KIM elastic response spectra are applied on the foundation baseplate and take into consideration incoherent earthquake ground motions, structural embedment, and soil scattered ground motions (soil with excavation). Frequency domain time history analysis performed on a comprehensive SSI model identified the stiff soil condition as the most penalizing with respect to the structural response. Resulting peak ground accelerations of the translational KIM spectra are compatible with the free-field soil surface ENSI-2015 UHS at an AEP of $10^{-4}/a$ (Figure 1).

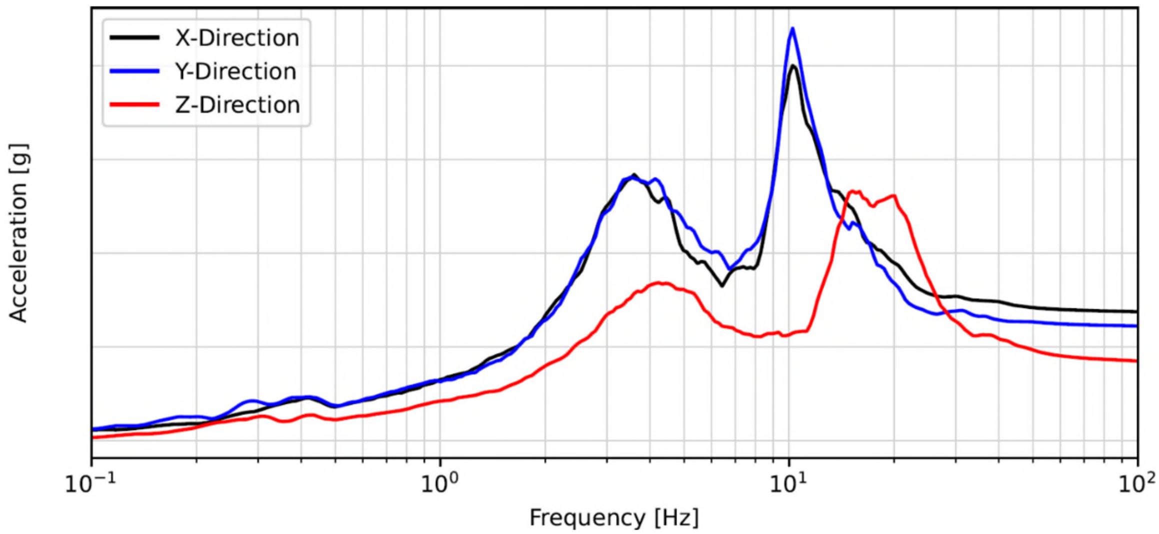

Figure 2. KIM translational elastic response spectra, averaged, 7% damping, stiff soil.

The aforementioned KIM response spectra are used as a seismic loading in the elastic response spectrum analysis and are combined with permanent and live loads within the earthquake load case combination (LCC). Ultimate limit state analysis (ULS) is performed in accordance with the SIA 262 (2003) standard to obtain the seismic demands and compare them against the available structural member capacities.

The global stability of the building is provided by the structural integrity of the cylindric exterior wall. The KIM spectra were scaled up to the level until the structural capacity of the exterior wall have been reached. Based on the results of the analysis two additional structural areas representative of the global structural resistance (Figure 3 and 4) are identified: basement walls on the foundation plate beneath the calotte including the central concrete core and the reinforced cylindrical internal structure protection wall above the reactor floor at level 18.4*m*.

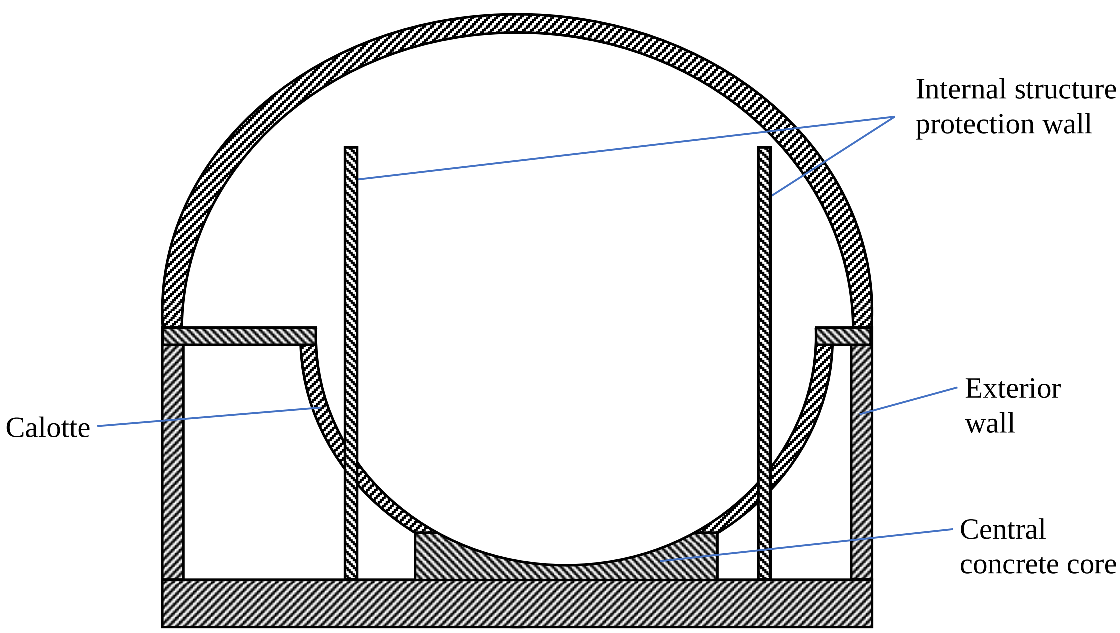

Figure 3. Reactor building critical members, vertical section cut.

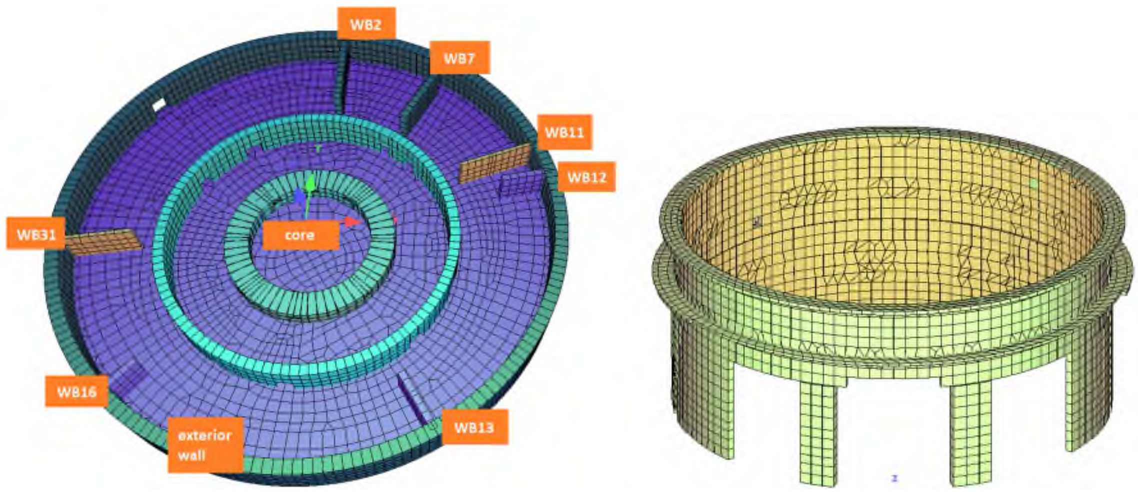

Figure 4. Relevant structural members: (left) Basement walls on the foundation plate beneath the calotte and (right) Upper part of the cylindrical internal structure protection wall at level 18.4*m*.

The available (capacity) and required (demand) reinforcement ratios in vertical and horizontal direction of the critical reinforced concrete basement walls and circular core resulting from the ULS analysis due to scaled RSA-based earthquake LCC are compared. The results are normalized to the capacity of the exterior cylindric wall. The capacity utilization (ratio of capacity to demand) in several structural members exceed 100%, see Table 1 and Figure 5. This is mostly due to horizontal earthquake loads and the onset of a load redistribution.

The overstresses due to lateral loading of the central concrete core and basement walls does not result in a global building failure mode since a redistribution of forces and moments to the rest of the internal and exterior walls takes place due to nonlinear concrete material behavior. In addition to that, inelastic energy dissipation resulting from the post-elastic deformation of the structural members would result in reduction of the elastic seismic demands. For these reasons, in the next stage, the nonlinear material behavior including local inelastic effects of the reinforced concrete elements in the basement and in the cylindrical wall above the reactor floor is taken into account to assess a realistic redistribution of the internal forces and moments.

Table 1: Relevant basement wall capacity utilization based on exterior wall normalized vertical capacity due to scaled RSA-based earthquake LLC.

Position	Capacity utilization	
	Vertical	Horizontal
WB 12	<100%	>100%
WB 13	>100%	>100%
WB 16	>100%	>100%
WB 2	<100%	>100%
WB 7	<100%	>100%
WB 31	>100%	>100%
WB 11	<100%	>100%
Exterior wall	**100%**	<100%

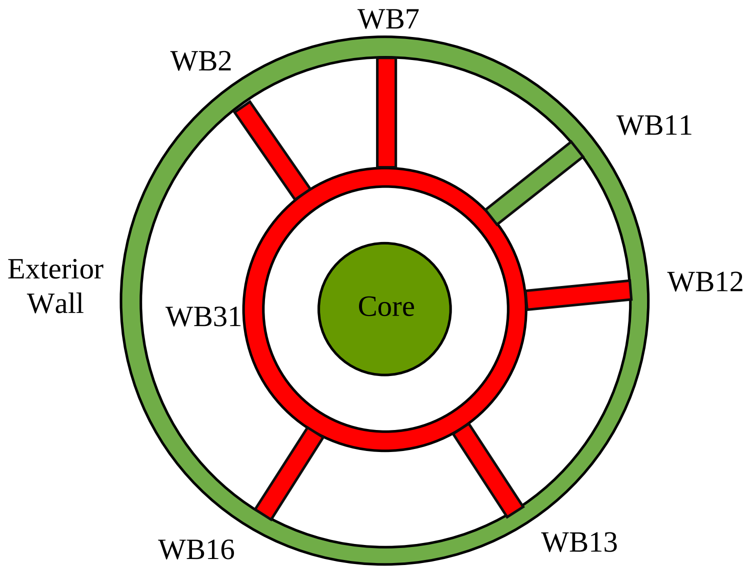

Figure 5. Response spectrum analysis results – selected basement walls to increase the seismic margin: exceeding (red) the structural capacity of the exterior wall (green).

NONLINEAR SEISMIC CAPACITY ANALYSIS

Structural failure in general occurs when the inelastic deformations of the structural members are large enough that it impairs the operability of critical equipment or when structural collapse happens as result of global loss of structural stability (e.g., soft story, etc.). In this particular study the failure can be characterized as the state when the relevant structural zones (see Figure 3) lose their lateral load bearing capacity resulting in large plastic material strains causing global structural collapse.

Failure of one or several walls in the building does not automatically constitute the failure of the entire structure. As the results of the elastic RSA-based analysis indicates, the structure possesses post-elastic capacity reserves. To properly assess the ultimate load bearing capacity of the structure, it is necessary to allow the structure to undergo post-elastic deformations, which will enable the redistribution of the forces from the areas experiencing large inelastic responses to the areas with smaller capacity utilization.

Several approaches, ranging from the most accurate nonlinear time history analysis to practical performance-based nonlinear static procedures (e.g., pushover analyses) have been critically assessed with respect to several criteria defined by the project. An optimal choice is made in utilizing the engineering-based nonlinear seismic capacity analysis using equivalent seismic static forces to assess the ultimate failure capacity of the structure.

Chosen approach is essentially a subset of the standard pushover analysis (see ATC-40 (1996), EN EN1998-1 (2004), Chopra and Goel (1999) and Fajfar (2000)). The main difference to a standard pushover analysis is that the reduction of the seismic demand accounting for the inelastic energy dissipation is not taken into consideration, leading to a more conservative approach. However, in the seismic fragility analysis and determination of the High-Confidence-of-Low-Probability-of-Failure (HCLPF) seismic capacity, the reduction of the seismic demand is taken into consideration using the inelastic energy absorption factor.

Figure 6 shows the nonlinear material definition of the structural members in the selected zones. Reinforced concrete walls have been modelled with layered shell elements and the nonlinear inelastic material steel and concrete constitutive model specified by the uniaxial compressive and tensile stress-strain curves shown in Figure 6, accounting also for the mechanical behavior in multiaxial stress states.

In case of the central concrete core, if it was to remain elastic, there would be almost no redistribution of the internal forces to surrounding walls due to the large core stiffness. Thus, the core is also allowed to behave inelastically by defining the ultimate limit horizontal force derived from the maximal shear force which is activated in the concrete joint by existing vertical reinforcement bars shown in Figure 6. Ultimate limit shear force in general comprises three parts (DIN 1045-1 (2008)): frictional resistance of the concrete, cohesion of the concrete, and shear resistance of the reinforcement in the concrete joint. Due to cyclic loading conditions and incremental increase of the concrete cracks, the two first terms have been neglected and the ultimate core shear resistance has been determined solely based on the reinforcement shear resistance. This behavior has been modelled using nonlinear prestressed frictional springs.

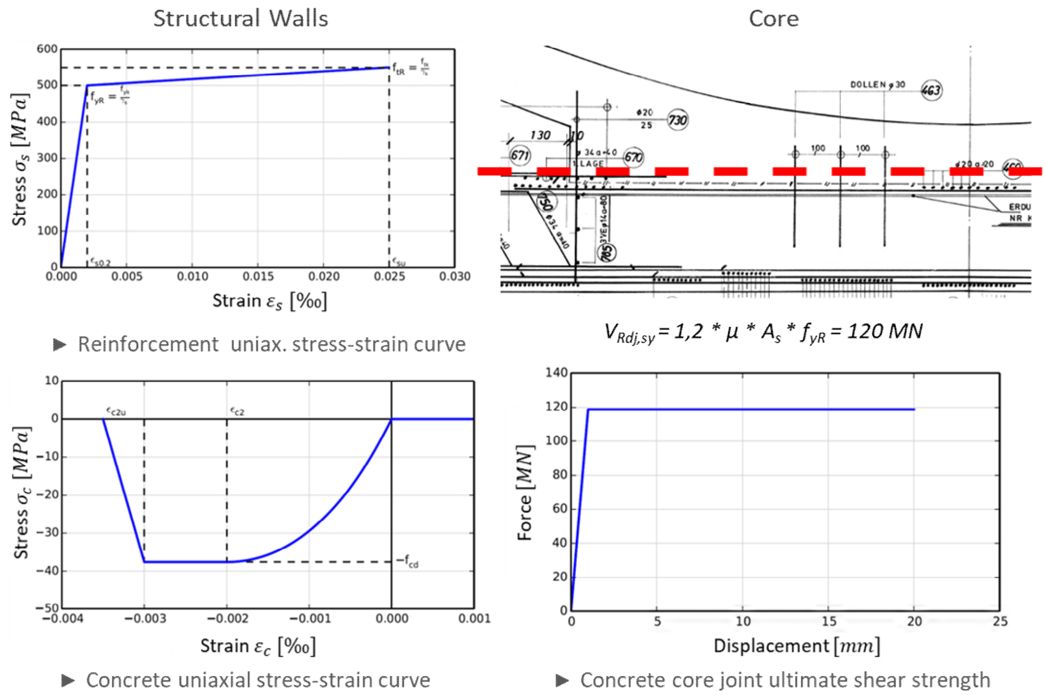

Figure 6. Nonlinear material definition of the relevant structural members.

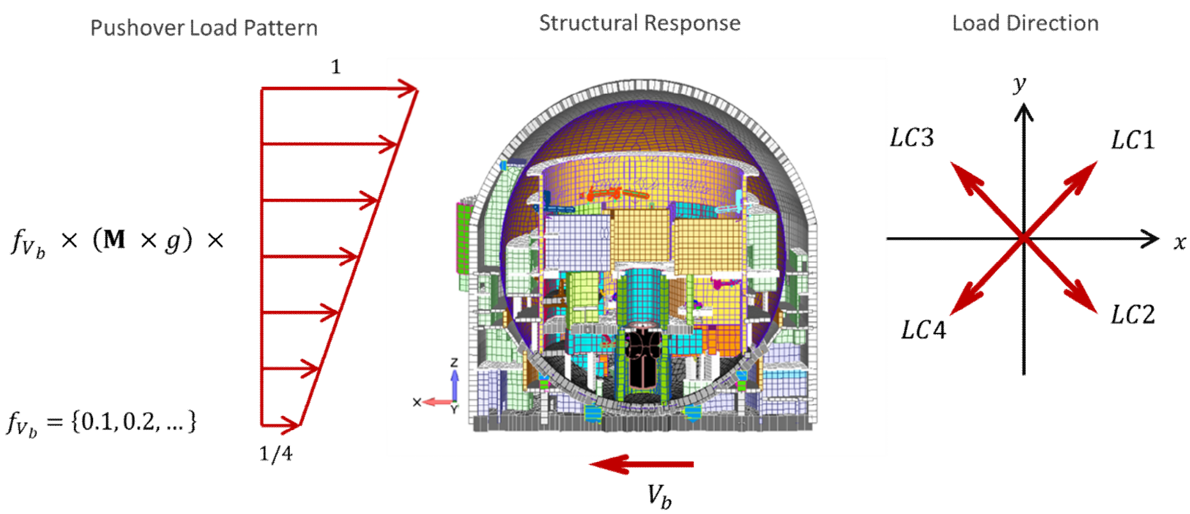

Figure 7. Pushover load definition.

Nonlinear static structural analysis is performed by subjecting the structure to a linearly increasing load pattern of lateral forces representing the pushover loads (see Figure 7). The pushover load, representing the acting forces that the structure would be experiencing when subjected to earthquake excitation, is defined trough equivalent mass-proportional static forces which vary linearly over the height with the acceleration ratio of 4 between the acceleration at the foundation plate and at the top of the containment (see Figure 7). This distribution is in good agreement with the distribution of the rigid body floor accelerations obtained within a separate detailed SSI analysis for the determination of floor response spectra. Four different load cases corresponding to four different governing earthquake directions were analyzed. The pushover load is incrementally scaled using the base shear scaling factor f_{Vb} until the ultimate structural capacity is reached.

As aforementioned in this study the global structural failure can be characterized as the state when the critical structural members lose their lateral load bearing capacity resulting in large lateral deformations causing structural collapse and/or critical equipment failure. On a local reinforced concrete structural member level, failure is defined by the maximal allowable reinforcement steel ($\varepsilon_{su} = 25$ ‰) and compressive concrete strains ($\varepsilon_{c1u} = 3.5$ ‰), see DIN 1045-1 (2008).

Figure 8 shows the seismic capacity curve in terms of the base shear parameter (scaling factor f_{Vb}) and a chosen damage parameter, including several characteristic levels. The representative damage parameter in this case is the maximal reinforcement strain ε_s corresponding to the maximal reinforcement strain of the exterior concrete wall.

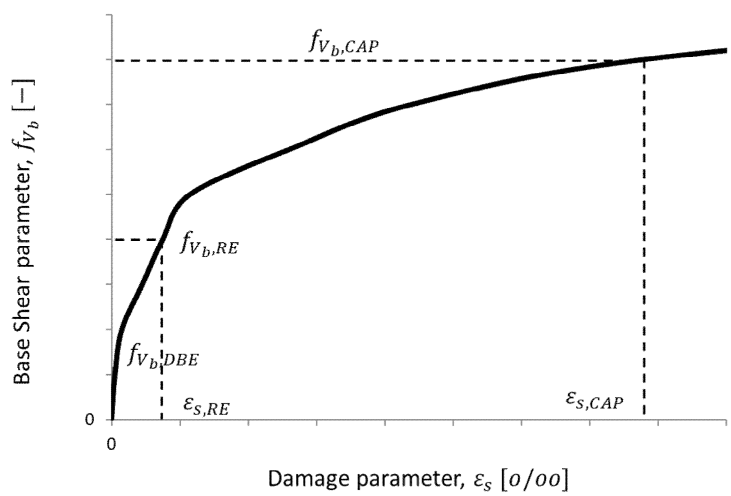

Figure 8. Seismic capacity curve with characteristic levels: DBE – original seismic hazard level used for the structural design, RE – new RLE, CAP – ultimate capacity level.

At the earthquake level corresponding to the base shear factor f_{Vb1} the shear capacity of the massive concrete core is reached (see Figure 6) and it represents the onset of the redistribution of the internal forces. In other words, further increase in the earthquake excitation results in the redistribution of the internal forces from the core to the remaining basement walls (see Figure 5).

At the Base shear factor f_{Vb2} damage to the relevant structural members in the selected zones is still low. For example, maximal reinforcement steel strains of the exterior wall (see Figure 9 (left)) and upper cylindrical internal structure protection wall (Figure 10 (left)) are 1.5 ‰ ($= \varepsilon_{s,RE}$) and 1.7 ‰, respectively, which is well below the elastic limit of the reinforcement steel of $\varepsilon_{s,y}$ $=2.4$ ‰. At this level of earthquake structural integrity, stability and safety are assured with acceptable damage to the structural members.

Base shear factor f_{Vb3} corresponds to the ultimate capacity level of the structure. At this earthquake level the maximal reinforcement steel strain corresponds to the maximal strain of the exterior wall and is equal to $15.6‰$ (Figure 9 (right)), whereas the corresponding maximal concrete compression strain of the exterior wall is $2.2‰$. Maximal reinforcement steel strain of the upper cylindrical wall is equal to $8.1‰$. Formation of plastic hinges at the bottom of the portal walls is clearly identifiable in Figure 10 (right). The strain values are below the limit strain values and the load carrying capacity of the structural members is still maintained.

Any increase of the earthquake excitation beyond the level of $f_{Vb,CAP} = f_{Vb3}$ results in the local failure of the critical structural members and extensive lateral displacements and 2nd order effects (see Figure 11). In this failure scenario, the exterior wall, which takes most of the loads from the load redistribution after the shear capacity of the concrete core has been reached, represents the "last line of defense" and the failure of this wall results in the loss of the lateral load bearing capacity, appearance of soft floor at the lowest structural level below the calotte, global loss of stability and ultimately the structural collapse. Therefore, the calculated base shear factor of f_{Vb3} determines the ultimate capacity level.

The structural response at the ultimate capacity level (f_{Vb3}) provides the bases for the seismic fragility analysis.

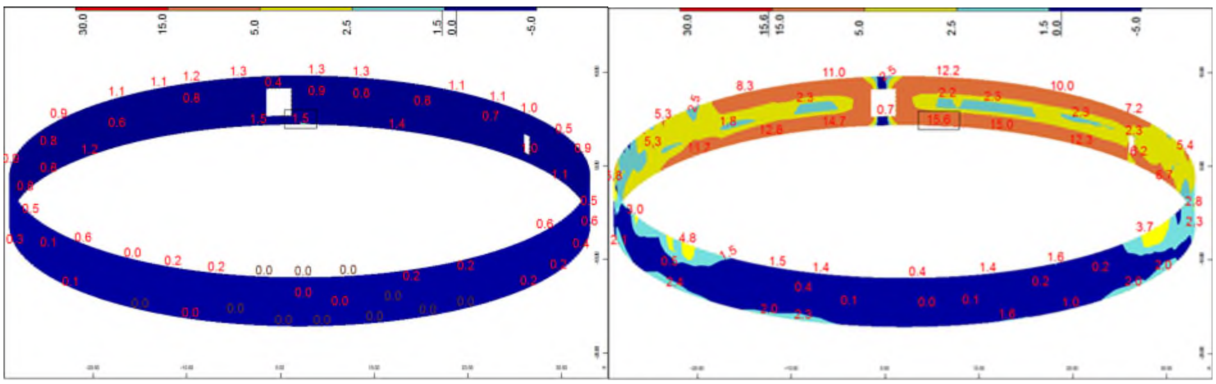

Figure 9. Seismic capacity analysis results, Exterior wall, Reinforcement strains [‰]: (left) Response at RE level, f_{Vb2} (right) Response at ultimate capacity level, f_{Vb3}.

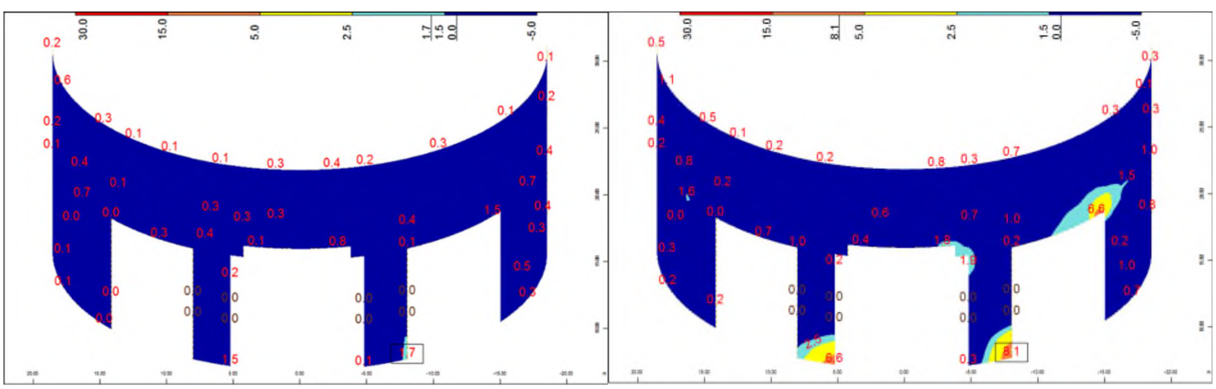

Figure 10. Seismic capacity analysis results, Upper cylindrical protection wall, Reinforcement strains [‰]: (left) Response at RE level f_{Vb2} (right) Response at ultimate capacity level f_{Vb3}.

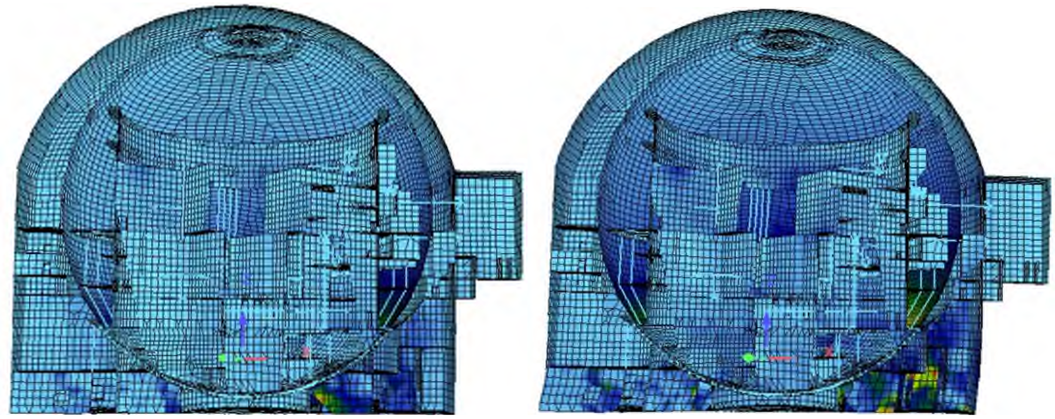

Figure 11. Seismic capacity analysis results, Global structural response, Deformation and stresses: (left) Response at RE level f_{Vb2} (right) Response at ultimate capacity level, f_{Vb3}.

SEISMIC FRAGILITY ANALYSIS

The analysis performed leading up to the fragility analysis provided preliminary risk insights that informed of a relatively large structural capacity against the RE seismic loadings. With the gained information, it is decided to approach the reactor building fragility analysis with risk significance in mind and utilize the hybrid method in accordance with EPRI 102988 (2002). This methodology is based on the calculation of a conservative deterministic failure margin (CDFM) HCLPF capacity. EPRI NP-6041-SL (1991) is used to develop the $\text{HCLPF}_{\text{CDFM}}$ referenced to the RE PGA.

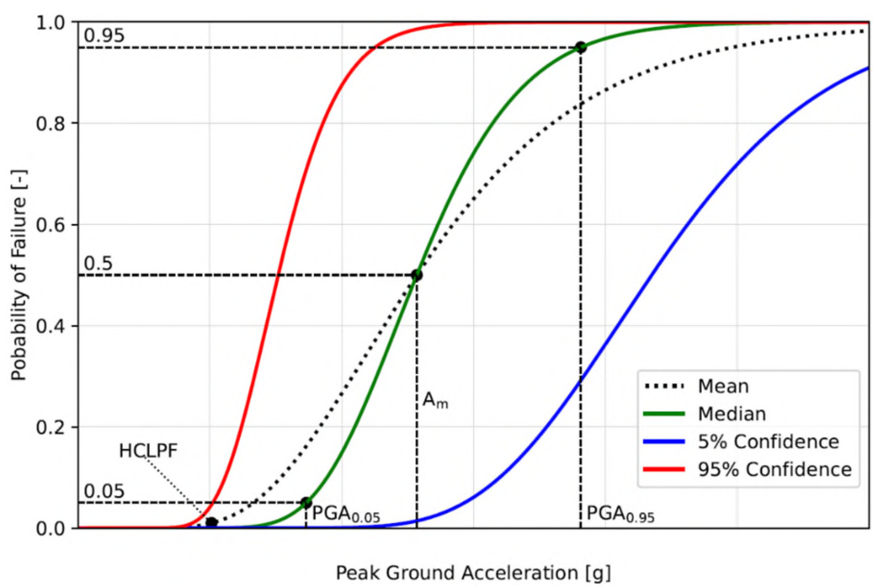

Figure 12. Gösgen reactor building fragility curves.

While other potential failure modes like the steel containment sliding on the concrete calotte, the upper internal structure protection wall capacity, reactor building sliding and overturning, adjacent building impact, and many more are evaluated, this paper focuses on the failure that is determined to be the ultimate failure mode. Hence, an elastic scale factor $FS_E = \varepsilon_{s,y} / \varepsilon_{s,RE}$ is developed for the exterior wall of the reactor building. Thereby, $\varepsilon_{s,y}$ is the elastic strain limit of the reinforcement steel in the exterior wall and

$\varepsilon_{s,RE}$ is the actual strain in the reinforcement due to the RE. In the next step the inelastic energy absorption factor F_μ is derived from the results of the nonlinear static seismic capacity analysis. This factor is conservatively calculated from the inelastic margin in between the structural responses of the exterior wall at its elastic limit and ultimate failure. With that, the inelastic scale factor $FS_I = FS_E \cdot F_\mu$ is determined and the HCLPF capacity is calculated.

With the HCLPF calculated the composite uncertainty β_c is estimated using EPRI 1025287 (2013). The median seismic capacity referenced to the RE PGA $A_m = HCLPF_{CDFM} \cdot e^{2.33\beta_c}$. Figure 12 shows the fragility curves for mean, median, 5%, and 95% confidence levels.

CONCLUSIONS

The RSA based seismic evaluation served as preliminary risk insight and identified some of the most relevant structural areas. Thereby, two prominent locations are the cylindrical reinforced concrete wall above the reactor floor and the basement walls including circular concrete core above the baseplate. The elastic shear stiffness of the central concrete core in the RSA calculation is governed by the core geometry. However, the local failure due to lateral loading of the central concrete core does not result in global building failure since a redistribution of forces and moments to the internal and exterior walls takes place. For this reason, the nonlinear material behavior including local plastic effects of the reinforced concrete elements in the basement and in the cylindrical wall above the reactor floor is taken into account to assess a realistic redistribution of the internal forces and moments.

The nonlinear static seismic capacity analysis is performed in accordance with DIN 1045-1 (2008). Thereby, the loading that simulates the seismic load case is incrementally scaled until the structural capacity is reached. The loading is defined through equivalent mass proportional static forces that vary vertically in agreement with the distribution of the floor acceleration. At the ENSI-2015 RLE for the site, which is 2.7 times larger than the original design basis earthquake, it is shown that large structural capacity margin exists in all the relevant structural members, which is significantly higher than the one calculated by the linear RSA-method. Performance at higher seismic hazard levels is characterized by the load redistribution from the concrete core to the basement walls with an increase of structural capacity by at least a factor of three.

A conservative hybrid method fragility analysis is performed for the reactor building resulting in a large HCLPF. The computed median seismic capacity referenced to the RE PGA using a generic composite uncertainty along with the corresponding HCLPF provides an efficient way to evaluate the reactor building risk significance in the SPRA.

REFERENCES

ATC-40. (1996). *Seismic Evaluation and Retrofit of Concrete Buildings*. Applied Technology Council. Redwood City, CA.

Chopra, A.K. and Goel, R.K. (1999). “Capacity-demand-diagram methods based on inelastic design spectrum”, *In: Earthquake Spectra 15.4, pp. 637–656*.

DIN 1045-1. (2008). *Tragwerke aus Beton, Stahlbeton und Spannbeton - Bemessung und Konstruktion Teil 1*.

EN1998-1:2004 (2004). *Eurocode 8: Design of structures for earthquake resistance, Part 1: General rules, seismic actions and rules for buildings*. CEN.

EPRI NP-6041-SL (1991). *A Methodology for Assessment of Nuclear Power Plant Seismic Margin (Rev. 1)*.

EPRI 102988 (2002). *Seismic Fragility Application Guide*.

EPRI 1025287 (2013). *Seismic Evaluation Guidance Screening, Prioritization and Implementation Details (SPID) for the Resolution of Fukushima Near-Term Task Force Recommendation 2.1: Seismic*.

Fajfar. P. (2000) “A Nonlinear Analysis Method for Performance-Based Seismic Design”. *In: Earthquake Spectra 16.3, pp. 573–592*.

SIA 262. (2003). *Betonbau*. Schweizer Norm.